Journal of Computational and Applied Mathematics 430 (2023) 115254

Contents lists available at ScienceDirect

Journal of Computational and Applied Mathematics

journal homepage: www.elsevier.com/locate/cam

Triquintic interpolation in three dimensions

Henry A. Boateng *, Kyle Bradach

Department of Mathematics, San Francisco State University, 1600 Holloway Avenue, San Francisco, 94132, CA, USA

ARTICLE INFO

Article history:
Received 20 October 2022
Received in revised form 3 April 2023

MSC:
65D05
65D15
65K05
65-04
70-08
76-04

Keywords:
Three-dimensional interpolation
Triquintic interpolation
Globally smooth interpolation

ABSTRACT

This paper develops a local triquintic interpolation method for a function defined over a unit cube mesh element. The resulting polynomial interpolant is isotropic and has global $\mathcal{C}^2$ continuity. The triquintic polynomial coefficients are related to the function and its derivatives at the eight corners of a mesh element by an invertible square matrix of rank 216. The proposed method is an extension of a previously developed tricubic interpolation scheme with global $\mathcal{C}^1$ continuity.

1. Introduction

Tricubic interpolation have been used very successfully in a range of fields, including ocean dynamics [1], plasma dynamics [2], image processing [3], particle physics [4], computational chemistry [5–7] and structural biology [8]. Lekien and Marsden (LM) [9] developed an isotropic tricubic interpolation scheme, defined on a rectilinear mesh, that did not separate the interpolant into a tensor product of three one-dimensional polynomials. Compared to the tensor product approach, the method due to LM has a reduced computational cost and provides easy access to more accurate derivatives. Lekien and Marsden also showed that their method has global $\mathcal{C}^1$ continuity but cannot achieve global $\mathcal{C}^2$ continuity. Thus, the interpolants for two adjacent meshes have the same function and first partial derivative values at the common face.

There is a need for higher order interpolants with a concomitant increase in smoothness. For example, it has been observed that, in particle simulations, the smoothness of the tricubic interpolation has an effect on the accuracy of the dynamics [2,6,7]. Additionally, in applications where second order derivatives of the interpolated kernel are required, such as in molecular dynamics simulations with dipoles, tricubic interpolation will not be very effective because of the lack of global $\mathcal{C}^2$ continuity.

This paper is a response to the need for higher order nontensorial interpolants. A search of the literature shows that triquintic interpolation has been implemented in cosmological simulations [10] and in fracture mechanics [11]. However, neither of these two works provide details about their implementation nor a study of the continuity and convergence properties of their interpolator. We extend the work of LM to systematically develop a triquintic interpolation method that is also isotropic. We prove that the method is globally $\mathcal{C}^2$ continuous but lacks global $\mathcal{C}^3$ continuity. We also prove that for a cubic mesh element of length x, the error for the tricubic interpolant decays uniformly as $\mathcal{O}(x^4)$ while the error

* Corresponding author.
E-mail addresses: boateng@sfsu.edu (H.A. Boateng), kbradach@mail.sfsu.edu (K. Bradach).

https://doi.org/10.1016/j.cam.2023.115254

for the triquintic interpolant decays uniformly as $\mathcal{O}(x^6)$. Finally, we provide numerical evidence of the decay rate of the errors and the accuracy of the tricubic and triquintic interpolations.

The paper is organized as follows. In Section 2 we describe the tricubic interpolation method developed by Lekien and Marsden [9]. We develop the triquintic interpolation method in Section 3. In Section 4, we prove that the triquintic method is globally $\mathcal{C}^2$ continues and that it lacks global $\mathcal{C}^3$ continuity. We derive the convergence rate of the interpolants supported by numerical evidence in Section 5 and summarize our conclusions in Section 6.

2. Tricubic interpolation

Let the function f be defined over a three dimensional rectilinear mesh. Then f is interpolated on and inside the unit cube mesh element (represented in Fig. 1) by the polynomial

$$\mathcal{P}(x,y,z) = \sum_{i,j,k=0}^{3} a_{ijk} x^i y^j z^k = \boldsymbol{\alpha}^T \boldsymbol{\mu}, \tag{1}$$

where the 64 unknown coefficients a_{ijk} are ordered into a vector $\boldsymbol{\alpha}$ by defining

$$\alpha_{1+i+4j+16k} = a_{ijk}, \qquad i,j,k = 0,1,2,3, \tag{2}$$

and the monomials $x^i y^j z^k$ are ordered into the vector $\boldsymbol{\mu}$ through a similar definition

$$\mu_{1+i+4j+16k} = x^i y^j z^j, \qquad i,j,k = 0,1,2,3. \tag{3}$$

To determine the 64 coefficients a_{ijk}, LM enforced the following 8 linearly independent constraints

$$\begin{Bmatrix} \mathcal{P} = f, \ \dfrac{\partial \mathcal{P}}{\partial x} = \dfrac{\partial f}{\partial x}, \ \dfrac{\partial \mathcal{P}}{\partial y} = \dfrac{\partial f}{\partial y}, \ \dfrac{\partial \mathcal{P}}{\partial z} = \dfrac{\partial f}{\partial z}, \\ \dfrac{\partial^2 \mathcal{P}}{\partial x \partial y} = \dfrac{\partial^2 f}{\partial x \partial y}, \ \dfrac{\partial^2 \mathcal{P}}{\partial x \partial z} = \dfrac{\partial^2 f}{\partial x \partial z}, \ \dfrac{\partial^2 \mathcal{P}}{\partial y \partial z} = \dfrac{\partial^2 f}{\partial y \partial z}, \ \dfrac{\partial^3 \mathcal{P}}{\partial x \partial y \partial z} = \dfrac{\partial^3 f}{\partial x \partial y \partial z} \end{Bmatrix}, \tag{4}$$

at the eight vertices of the unit cube to generate a full rank sparse linear system

$$B\boldsymbol{\alpha} = \boldsymbol{b}. \tag{5}$$

Here B is the 64×64 invertible coefficient matrix generated by applying the constraints to the polynomial and $\boldsymbol{b}$ is obtained from applying the constraints to the function. This choice of constraints is the only set that yields an isotropic interpolant with global $\mathcal{C}^1$ continuity. The coefficient vector is computed explicitly as $\boldsymbol{\alpha} = B^{-1}\boldsymbol{b}$. The matrix B^{-1} is independent of the function being interpolated and can be stored to be reused for different evaluation points within the mesh and for different functions. This feature is the main reason why the LM tricubic has less computational cost compared to the tensor product version.

3. Triquintic interpolation

The triquintic interpolant is defined over the same unit cube, depicted in Fig. 1, as the tricubic. A function f is represented locally on and inside the unit cube by the polynomial

$$\mathcal{P}(x,y,z) = \sum_{i,j,k=0}^{5} a_{ijk} x^i y^j z^k = \boldsymbol{\alpha}^T \boldsymbol{\mu}. \tag{6}$$

The elements of the vector $\boldsymbol{\alpha}$ are given by

$$\alpha_{1+i+6j+36k} = a_{ijk}, \qquad i,j,k = 0,1,2,3,4,5, \tag{7}$$

and the elements of the vector $\boldsymbol{\mu}$ are similarly ordered as

$$\mu_{1+i+6j+36k} = x^i y^j z^k, \qquad i,j,k = 0,1,2,3,4,5. \tag{8}$$

We need 216 linearly independent constraints to determine the 216 coefficients a_{ijk}. Following LM [9], our constraints will be defined at the eight vertices of the unit cube. Thus we require 27 constraints repeated at each vertex. We would like the interpolant to be isotropic and to achieve global $\mathcal{C}^2$ continuity.

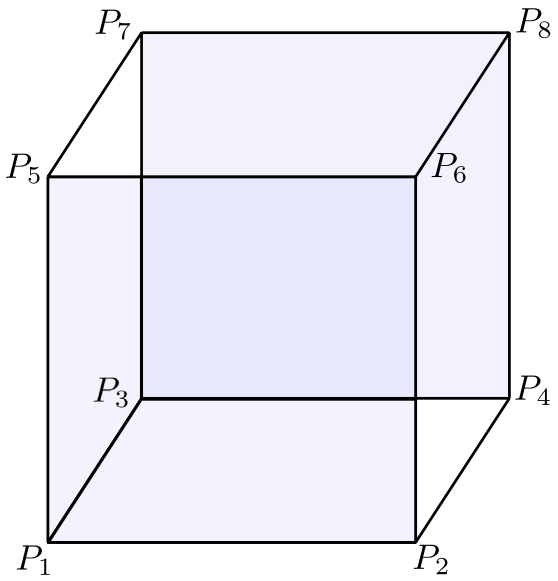

Fig. 1. The unit cube mesh element.

3.1. Constraints for triquintic interpolation

Because we want the interpolant to be at least globally C^2 continuous, the function and all its first and second derivatives must agree with the polynomial at the vertices of the cube which leads to the 10 constraints

$$\left\{ \mathcal{P} = f,\ \frac{\partial \mathcal{P}}{\partial x} = \frac{\partial f}{\partial x},\ \frac{\partial \mathcal{P}}{\partial y} = \frac{\partial f}{\partial y},\ \frac{\partial \mathcal{P}}{\partial z} = \frac{\partial f}{\partial z}, \right. \tag{9}$$
$$\left. \frac{\partial^2 \mathcal{P}}{\partial x^2} = \frac{\partial^2 f}{\partial x^2},\ \frac{\partial^2 \mathcal{P}}{\partial x \partial y} = \frac{\partial^2 f}{\partial x \partial y},\ \frac{\partial^2 \mathcal{P}}{\partial x \partial z} = \frac{\partial^2 f}{\partial x \partial z},\ \frac{\partial^2 \mathcal{P}}{\partial y^2} = \frac{\partial^2 f}{\partial y^2},\ \frac{\partial^2 \mathcal{P}}{\partial y \partial z} = \frac{\partial^2 f}{\partial y \partial z},\ \frac{\partial^2 \mathcal{P}}{\partial z^2} = \frac{\partial^2 f}{\partial z^2} \right\}.$$

Next, we match the third derivatives. First, we note that along any axis, the triquintic interpolant is just a fifth degree spline whose 6 coefficients are uniquely determined by the value of the function and its first and second derivatives at the endpoints of the interval. As such, constraints involving derivatives of the form

$$\frac{\partial^\nu \mathcal{P}}{\partial s^\nu}, \qquad \nu \geq 3, \qquad s \in \{x, y, z\}, \tag{10}$$

are dependent on the function and its first and second derivatives and thus are extraneous. As an example, consider the interpolant along the x-axis ($y = z = 0$),

$$\mathcal{P}(x, 0, 0) = \sum_{i=0}^{5} a_{i00} x^i = a_{000} + a_{100}x + a_{200}x^2 + a_{300}x^3 + a_{400}x^4 + a_{500}x^5, \tag{11}$$

$$\frac{\partial \mathcal{P}}{\partial x} = \sum_{i=i}^{5} i a_{i00} x^{i-1} = a_{100} + 2a_{200}x + 3a_{300}x^2 + 4a_{400}x^3 + 5a_{500}x^4, \tag{12}$$

$$\frac{\partial^2 \mathcal{P}}{\partial x^2} = \sum_{i=2}^{5} i(i-1) a_{i00} x^{i-2} = 2a_{200} + 6a_{300}x + 12a_{400}x^2 + 20a_{500}x^3, \tag{13}$$

$$\frac{\partial^3 \mathcal{P}}{\partial x^3} = \sum_{i=3}^{5} i(i-1)(i-2) a_{i00} x^{i-3} = 6a_{300} + 24a_{400}x + 60a_{500}x^2. \tag{14}$$

Evaluating Eqs. (11) to (14) at the left and right endpoints of the spline interval, $P_1 = (0, 0, 0)$ and $P_2 = (1, 0, 0)$ respectively, we get

$$\mathcal{P}\Big|_{(0,0,0)} = a_{000}, \quad \frac{\partial \mathcal{P}}{\partial x}\Big|_{(0,0,0)} = a_{100}, \quad \frac{\partial^2 \mathcal{P}}{\partial x^2}\Big|_{(0,0,0)} = 2a_{200}, \quad \frac{\partial^3 \mathcal{P}}{\partial x^3}\Big|_{(0,0,0)} = 6a_{300}, \tag{15}$$

$$\mathcal{P}\Big|_{(1,0,0)} = a_{000} + a_{100} + a_{200} + a_{300} + a_{400} + a_{500}, \tag{16}$$

$$\frac{\partial \mathcal{P}}{\partial x}\Big|_{(1,0,0)} = a_{100} + 2a_{200} + 3a_{300} + 4a_{400} + 5a_{500}, \tag{17}$$

$$\frac{\partial^2 \mathcal{P}}{\partial x^2}\Big|_{(1,0,0)} = 2a_{200} + 6a_{300} + 12a_{400} + 20a_{500}, \tag{18}$$

$$\frac{\partial^3 \mathcal{P}}{\partial x^3}\Big|_{(1,0,0)} = 6a_{300} + 24a_{400} + 60a_{500}. \tag{19}$$

We observe that

$$\begin{aligned}\frac{\partial^3 \mathcal{P}}{\partial x^3}\Big|_{(0,0,0)} = &-60\mathcal{P}\Big|_{(0,0,0)} + 60\mathcal{P}\Big|_{(1,0,0)} - 36\frac{\partial \mathcal{P}}{\partial x}\Big|_{(0,0,0)} - 24\frac{\partial \mathcal{P}}{\partial x}\Big|_{(1,0,0)} \\ &- 9\frac{\partial^2 \mathcal{P}}{\partial x^2}\Big|_{(0,0,0)} + 3\frac{\partial^2 \mathcal{P}}{\partial x^2}\Big|_{(1,0,0)},\end{aligned} \tag{20}$$

and

$$\begin{aligned}\frac{\partial^3 \mathcal{P}}{\partial x^3}\Big|_{(1,0,0)} = &-60\mathcal{P}\Big|_{(0,0,0)} + 60\mathcal{P}\Big|_{(1,0,0)} - 24\frac{\partial \mathcal{P}}{\partial x}\Big|_{(0,0,0)} - 36\frac{\partial \mathcal{P}}{\partial x}\Big|_{(1,0,0)} \\ &- 3\frac{\partial^2 \mathcal{P}}{\partial x^2}\Big|_{(0,0,0)} + 9\frac{\partial^2 \mathcal{P}}{\partial x^2}\Big|_{(1,0,0)},\end{aligned} \tag{21}$$

thus we omit the constraint $\frac{\partial^3 \mathcal{P}}{\partial x^3} = \frac{\partial^3 f}{\partial x^3}$. Similarly, by symmetry, we omit the constraints $\frac{\partial^3 \mathcal{P}}{\partial y^3} = \frac{\partial^3 f}{\partial y^3}$ and $\frac{\partial^3 \mathcal{P}}{\partial z^3} = \frac{\partial^3 f}{\partial z^3}$. The remaining set of third derivatives provide the 7 constraints

$$\begin{Bmatrix} \frac{\partial^3 \mathcal{P}}{\partial x^2 \partial y} = \frac{\partial^3 f}{\partial x^2 \partial y}, \ \frac{\partial^3 \mathcal{P}}{\partial x^2 \partial z} = \frac{\partial^3 f}{\partial x^2 \partial z}, \ \frac{\partial^3 \mathcal{P}}{\partial x \partial y^2} = \frac{\partial^3 f}{\partial x \partial y^2}, \\ \frac{\partial^3 \mathcal{P}}{\partial x \partial y \partial z} = \frac{\partial^3 f}{\partial x \partial y \partial z}, \ \frac{\partial^3 \mathcal{P}}{\partial y^2 \partial z} = \frac{\partial^3 f}{\partial y^2 \partial z}, \ \frac{\partial^3 \mathcal{P}}{\partial x \partial z^2} = \frac{\partial^3 f}{\partial x \partial z^2}, \ \frac{\partial^3 \mathcal{P}}{\partial y \partial z^2} = \frac{\partial^3 f}{\partial y \partial z^2} \end{Bmatrix}, \tag{22}$$

which are invariant under a rotation of the axis and thus maintain the isotropic property. The final 10 constraints are given by the fourth, fifth and sixth order derivatives which do not involve derivatives of the form given in Eq. (10). These 10 constraints are

$$\begin{Bmatrix} \frac{\partial^4 \mathcal{P}}{\partial x^2 \partial y^2} = \frac{\partial^4 f}{\partial x^2 \partial y^2}, \ \frac{\partial^4 \mathcal{P}}{\partial x^2 \partial z^2} = \frac{\partial^4 f}{\partial x^2 \partial z^2}, \ \frac{\partial^4 \mathcal{P}}{\partial y^2 \partial z^2} = \frac{\partial^4 f}{\partial y^2 \partial z^2}, \\ \frac{\partial^4 \mathcal{P}}{\partial x^2 \partial y \partial z} = \frac{\partial^4 f}{\partial x^2 \partial y \partial z}, \ \frac{\partial^4 \mathcal{P}}{\partial x \partial y^2 \partial z} = \frac{\partial^4 f}{\partial x \partial y^2 \partial z}, \ \frac{\partial^4 \mathcal{P}}{\partial x \partial y \partial z^2} = \frac{\partial^4 f}{\partial x \partial y \partial z^2} \end{Bmatrix}, \tag{23}$$

$$\left\{ \frac{\partial^5 \mathcal{P}}{\partial x^2 \partial y^2 \partial z} = \frac{\partial^5 f}{\partial x^2 \partial y^2 \partial z}, \ \frac{\partial^5 \mathcal{P}}{\partial x^2 \partial y \partial z^2} = \frac{\partial^5 f}{\partial x^2 \partial y \partial z^2}, \ \frac{\partial^5 \mathcal{P}}{\partial x \partial y^2 \partial z^2} = \frac{\partial^5 f}{\partial x \partial y^2 \partial z^2} \right\}, \tag{24}$$

and

$$\left\{ \frac{\partial^6 \mathcal{P}}{\partial x^2 \partial y^2 \partial z^2} = \frac{\partial^5 f}{\partial x^2 \partial y^2 \partial z^2} \right\}. \tag{25}$$

These last 10 constraints are also invariant under axis rotation, thus the interpolant is isotropic.

3.2. The triquintic linear system

To determine the 216 coefficients, the 27 constraints are enforced at the eight vertices of the cube, $P_1, \ldots, P_8$ to generate the full rank system defined in Eq. (5). We order the elements b_i in vector $\boldsymbol{b}$, and hence the rows of matrix

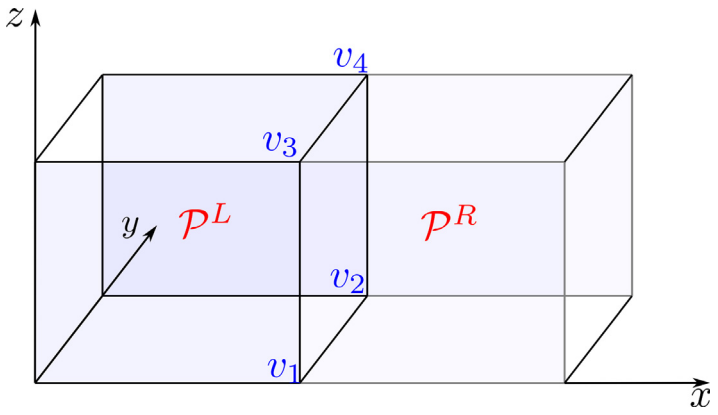

Fig. 2. Adjacent mesh elements.

B, by defining

$$b_i = \begin{cases} f(P_i), & 1 \le i \le 8, \quad \frac{\partial^2 f(P_{i-72})}{\partial z^2}, & 73 \le i \le 80, \quad \frac{\partial^4 f(P_{i-144})}{\partial x^2 \partial z^2}, & 145 \le i \le 152 \\ \frac{\partial f(P_{i-8})}{\partial x}, & 9 \le i \le 16, \quad \frac{\partial^3 f(P_{i-80})}{\partial x^2 \partial y}, & 81 \le i \le 88, \quad \frac{\partial^4 f(P_{i-152})}{\partial y^2 \partial z^2}, & 153 \le i \le 160 \\ \frac{\partial f(P_{i-16})}{\partial y}, & 17 \le i \le 24, \quad \frac{\partial^3 f(P_{i-88}),}{\partial x^2 \partial z}, & 89 \le i \le 96, \quad \frac{\partial^4 f(P_{i-160})}{\partial x^2 \partial y \partial z}, & 161 \le i \le 168 \\ \frac{\partial f(P_{i-24})}{\partial z}, & 25 \le i \le 32, \quad \frac{\partial^3 f(P_{i-96})}{\partial x \partial y^2}, & 97 \le i \le 104, \quad \frac{\partial^4 f(P_{i-168})}{\partial x \partial y^2 \partial z}, & 169 \le i \le 176 \\ \frac{\partial^2 f(P_{i-32})}{\partial x^2}, & 33 \le i \le 40, \quad \frac{\partial^3 f(P_{i-104})}{\partial x \partial y \partial z}, & 105 \le i \le 112, \quad \frac{\partial^4 f(P_{i-176})}{\partial x \partial y \partial z^2}, & 177 \le i \le 184 \\ \frac{\partial^2 f(P_{i-40})}{\partial x \partial y}, & 41 \le i \le 48, \quad \frac{\partial^3 f(P_{i-112})}{\partial y^2 \partial z}, & 113 \le i \le 120, \quad \frac{\partial^5 f(P_{i-184})}{\partial x^2 \partial y^2 \partial z}, & 185 \le i \le 192 \\ \frac{\partial^2 f(P_{i-48})}{\partial x \partial z}, & 49 \le i \le 56, \quad \frac{\partial^3 f(P_{i-120})}{\partial x \partial z^2}, & 121 \le i \le 128, \quad \frac{\partial^5 f(P_{i-192})}{\partial x^2 \partial y \partial z^2}, & 193 \le i \le 200 \\ \frac{\partial^2 f(P_{i-56})}{\partial y^2}, & 57 \le i \le 64, \quad \frac{\partial^3 f(P_{i-128})}{\partial y \partial z^2}, & 129 \le i \le 136, \quad \frac{\partial^5 f(P_{i-200})}{\partial x \partial y^2 \partial z^2}, & 201 \le i \le 208 \\ \frac{\partial^2 f(P_{i-64})}{\partial y \partial z}, & 65 \le i \le 72, \quad \frac{\partial^4 f(P_{i-136})}{\partial x^2 \partial y^2}, & 137 \le i \le 144, \quad \frac{\partial^6 f(P_{i-208})}{\partial x^2 \partial y^2 \partial z^2}, & 209 \le i \le 216 \end{cases} \tag{26}$$

We solve for the coefficients as $\boldsymbol{\alpha} = B^{-1}\boldsymbol{b}$ and the polynomial defined in Eq. (6) becomes

$$\mathcal{P}(x, y, z) = \boldsymbol{b}^T \left(B^{-1}\right)^T \boldsymbol{\mu}. \tag{27}$$

The matrix B^{-1} is sparse with 9261 non-zero elements. Because the matrix depends only on the unit cube mesh and not on the function being interpolated, it is stored and reused. The scaled matrix $8B^{-1}$ is available online [12].

4. Smoothness property of the isotropic triquintic interpolant

Now, we study the smoothness property of the triquintic interpolant. First, we prove that the interpolant has global $\mathcal{C}^2$ continuity. Then we show that global $\mathcal{C}^3$ continuity does not hold for the triquintic interpolant. The triquintic polynomial interpolant $\mathcal{P}(x, yz)$ is $\mathcal{C}^\infty$ inside any mesh element and as such, its global smoothness is determined by the smoothness properties at the boundary of each mesh element. Following LM, we will focus our analysis on the common boundary(face) (v_1, v_3, v_4, v_2) between two adjacent mesh elements in Fig. 2. By symmetry, the analysis will apply to the other faces.

4.1. Proof of global $\mathcal{C}^2$ continuity

Lemma 1. *The triquintic interpolant $\mathcal{P}$ is everywhere continuous.*

Proof. Consider the adjacent mesh elements in Fig. 2 and their boundary (v_1, v_3, v_4, v_2). Our goal is to show that at the boundary (v_1, v_3, v_4, v_2), the interpolant in the left mesh element, $\mathcal{P}^L$, is equal to the interpolant in the right mesh element, $\mathcal{P}^R$, which is sufficient to prove continuity across the boundary.

For $\mathcal{P}^L$, $x = 1$ at the boundary, thus

$$\mathcal{P}^L(1, y, z) = \sum_{j,k=0}^{5} \left(\sum_{i=0}^{5} a_{ijk} \right) y^j z^k = \left(\boldsymbol{\alpha}^L\right)^T \boldsymbol{\mu}^L, \tag{28}$$

where the elements of vector $\boldsymbol{\alpha}^L$ are ordered as

$$\alpha^L_{1+j+6k} = \sum_{i=0}^{5} a_{ijk}, \qquad j, k = 0, 1, 2, 3, 4, 5, \tag{29}$$

and the elements of vector $\boldsymbol{\mu}^L$ are similarly ordered as

$$\mu^L_{1+j+6k} = y^j z^k, \qquad j, k = 0, 1, 2, 3, 4, 5. \tag{30}$$

For $\mathcal{P}^R$, $x = 0$ at the boundary, hence

$$\mathcal{P}^R(0, y, z) = \sum_{j,k=0}^{5} a_{0jk} y^j z^k = \left(\boldsymbol{\alpha}^R\right)^T \boldsymbol{\mu}^R, \tag{31}$$

with the elements of vectors $\boldsymbol{\alpha}^R$ and $\boldsymbol{\mu}^R$ ordered as

$$\alpha^R_{1+j+6k} = a_{0jk}, \qquad j, k = 0, 1, 2, 3, 4, 5, \tag{32}$$

and

$$\mu^R_{1+j+6k} = y^j z^k, \qquad j, k = 0, 1, 2, 3, 4, 5, \tag{33}$$

respectively. Now notice that $\boldsymbol{\mu}^L = \boldsymbol{\mu}^R$, thus to show that $\mathcal{P}^L = \mathcal{P}^R$ on the boundary, we only need to show that $\boldsymbol{\alpha}^L = \boldsymbol{\alpha}^R$. We solve for $\boldsymbol{\alpha}^L$ from the linear system

$$B^L \boldsymbol{\alpha}^L = \boldsymbol{b}^L, \tag{34}$$

and for $\boldsymbol{\alpha}^R$ from the linear system

$$B^R \boldsymbol{\alpha}^R = \boldsymbol{b}^R. \tag{35}$$

At the four vertices $\{v_1, v_2, v_3, v_4\}$, we enforce the subset of the original 27 set of constraints

$$\begin{Bmatrix} \mathcal{P} = f, \ \dfrac{\partial \mathcal{P}}{\partial y} = \dfrac{\partial f}{\partial y}, \ \dfrac{\partial \mathcal{P}}{\partial z} = \dfrac{\partial f}{\partial z}, \ \dfrac{\partial^2 \mathcal{P}}{\partial y^2} = \dfrac{\partial^2 f}{\partial y^2}, \ \dfrac{\partial^2 \mathcal{P}}{\partial y \partial z} = \dfrac{\partial^2 f}{\partial y \partial z}, \\ \dfrac{\partial^2 \mathcal{P}}{\partial z^2} = \dfrac{\partial^2 f}{\partial z^2}, \ \dfrac{\partial^3 \mathcal{P}}{\partial y^2 \partial z} = \dfrac{\partial^3 f}{\partial y^2 \partial z}, \ \dfrac{\partial^3 \mathcal{P}}{\partial y \partial z^2} = \dfrac{\partial^3 f}{\partial y \partial z^2}, \ \dfrac{\partial^4 \mathcal{P}}{\partial y^2 \partial z^2} = \dfrac{\partial^4 f}{\partial y^2 \partial z^2} \end{Bmatrix}. \tag{36}$$

which do not involve derivatives in x. These 9 constraints remain linearly independent since the larger set is linearly independent [13]. Because $\boldsymbol{\mu}^L = \boldsymbol{\mu}^R$, and the constraints are the same for both $\mathcal{P}^L$ and $\mathcal{P}^R$, the coefficient matrices B^L and B^R in Eqs. (34) and (35) respectively, are the same (see Ref. [14] for the coefficient matrix). In addition, the right-hand

sides $\boldsymbol{b}^L$ and $\boldsymbol{b}^R$ depend only on the data f, as such

$$\boldsymbol{b}^L = \boldsymbol{b}^R = \begin{cases} f(v_i), & 1 \le i \le 4 \\ \dfrac{\partial f}{\partial y}(v_{i-4}), & 5 \le i \le 8 \\ \dfrac{\partial f}{\partial z}(v_{i-8}), & 9 \le i \le 12 \\ \dfrac{\partial^2 f}{\partial y^2}(v_{i-12}), & 13 \le i \le 16 \\ \dfrac{\partial^2 f}{\partial y \partial z}(v_{i-16}), & 17 \le i \le 20 \\ \dfrac{\partial^2 f}{\partial z^2}(v_{i-20}), & 21 \le i \le 24 \\ \dfrac{\partial^3 f}{\partial y^2 \partial z}(v_{i-24}), & 25 \le i \le 28 \\ \dfrac{\partial^3 f}{\partial y \partial z^2}(v_{i-28}), & 29 \le i \le 32 \\ \dfrac{\partial^4 f}{\partial y^2 \partial z^2}(v_{i-32}), & 33 \le i \le 36 \end{cases} \tag{37}$$

It follows then that

$$\boldsymbol{\alpha}^L = \left(B^L\right)^{-1} \boldsymbol{b}^L = \left(B^R\right)^{-1} \boldsymbol{b}^R = \boldsymbol{\alpha}^R, \tag{38}$$

hence $\mathcal{P}^L = \mathcal{P}^R$ and thus the interpolant is continuous across the boundary. Similar arguments for y and z, lead to the conclusion that the interpolant is continuous everywhere. □

Lemma 2. *Derivatives of the form*

$$\frac{\partial^{\gamma+\nu}\mathcal{P}}{\partial y^\gamma \partial z^\nu}, \qquad \gamma + \nu = 1, 2, 3, 4, 5, 6,$$

are continuous on the mesh element boundaries perpendicular to the x-axis.

Proof. From Lemma 1, $\mathcal{P}^L = \mathcal{P}^R$ on the boundary, (v_1, v_3, v_4, v_2). Since the interpolants are polynomials in y and z, this means that their derivatives match to any order on the boundary. But (v_1, v_3, v_4, v_2) is an arbitrary boundary perpendicular to the x-axis, thus,

$$\frac{\partial^{\gamma+\nu}\mathcal{P}^L}{\partial y^\gamma \partial z^\nu} = \frac{\partial^{\gamma+\nu}\mathcal{P}^R}{\partial y^\gamma \partial z^\nu}, \qquad \text{for } \gamma + \nu = 1, 2, 3, 4, 5, 6, \tag{39}$$

on mesh boundaries perpendicular to the x-axis. □

Corollary 2.1. *Derivatives of the form*

$$\frac{\partial^{\gamma+\nu}\mathcal{P}}{\partial x^\gamma \partial y^\nu}, \qquad \gamma + \nu = 1, 2, 3, 4, 5, 6,$$

are continuous on the mesh element boundaries perpendicular to the z-axis while derivatives of the form

$$\frac{\partial^{\gamma+\nu}\mathcal{P}}{\partial x^\gamma \partial z^\nu}, \qquad \gamma + \nu = 1, 2, 3, 4, 5, 6,$$

are continuous on the mesh element boundaries perpendicular to the y-axis.

Proof. The corollary follows from Lemma 1 and from Lemma 2 by symmetry. □

Lemma 3. *The polynomial* $\frac{\partial \mathcal{P}}{\partial x}$ *is continuous on the boundary* (v_1, v_3, v_4, v_2).

Proof. Just as in the proof of Lemma 1, it suffices to show that $\frac{\partial \mathcal{P}^L}{\partial x}(1, y, z) = \frac{\partial \mathcal{P}^R}{\partial x}(0, y, z)$. We start by differentiating $\mathcal{P}$ with respect to x to get

$$\frac{\partial \mathcal{P}}{\partial x}(x, y, z) = \sum_{j,k=0}^{5} \sum_{i=1}^{5} i a_{ijk} x^{i-1} y^j z^k. \tag{40}$$

On the boundary,

$$\frac{\partial \mathcal{P}^L}{\partial x}(1,y,z) = \sum_{j,k=0}^{5}\left(\sum_{i=1}^{5} i a_{ijk}\right) y^j z^k = \left(\boldsymbol{\alpha}^L\right)^T \boldsymbol{\mu}^L, \tag{41}$$

where

$$\alpha^L_{1+j+6k} = \sum_{i=1}^{5} i a_{ijk}, \qquad j,k = 0,1,2,3,4,5, \tag{42}$$

and

$$\frac{\partial \mathcal{P}^R}{\partial x}(0,y,z) = \sum_{j,k=0}^{5} a_{1jk}\, y^j z^k = \left(\boldsymbol{\alpha}^R\right)^T \boldsymbol{\mu}^R, \tag{43}$$

with

$$\alpha^R_{1+j+6k} = a_{1jk}, \qquad j,k = 0,1,2,3,4,5, \tag{44}$$

and

$$\mu^L_{1+j+6k} = \mu^R_{1+j+6k} = y^j z^k, \qquad j,k = 0,1,2,3,4,5. \tag{45}$$

Again, we have $\boldsymbol{\mu}^L = \boldsymbol{\mu}^R$, hence we only need to show that $\boldsymbol{\alpha}^L = \boldsymbol{\alpha}^R$. At the four vertices $\{v_1, v_2, v_3, v_4\}$, we enforce the following subset of the original set of constraints

$$\left\{ \begin{array}{l} \dfrac{\partial \mathcal{P}}{\partial x} = \dfrac{\partial f}{\partial x},\ \dfrac{\partial^2 \mathcal{P}}{\partial x \partial y} = \dfrac{\partial^2 f}{\partial x \partial y},\ \dfrac{\partial^2 \mathcal{P}}{\partial x \partial z} = \dfrac{\partial^2 f}{\partial x \partial z},\ \dfrac{\partial^3 \mathcal{P}}{\partial x \partial y^2} = \dfrac{\partial^3 f}{\partial x \partial y^2},\ \dfrac{\partial^3 \mathcal{P}}{\partial x \partial y \partial z} = \dfrac{\partial^3 f}{\partial x \partial y \partial z}, \\ \dfrac{\partial^3 \mathcal{P}}{\partial x \partial z^2} = \dfrac{\partial^3 f}{\partial x \partial z^2},\ \dfrac{\partial^4 \mathcal{P}}{\partial x \partial y^2 \partial z} = \dfrac{\partial^4 f}{\partial x \partial y^2 \partial z},\ \dfrac{\partial^4 \mathcal{P}}{\partial x \partial y \partial z^2} = \dfrac{\partial^4 f}{\partial x \partial y \partial z^2},\ \dfrac{\partial^5 \mathcal{P}}{\partial x \partial y^2 \partial z^2} = \dfrac{\partial^5 f}{\partial x \partial y^2 \partial z^2} \end{array} \right\}. \tag{46}$$

which involve just a single derivative in x. This leads to the same coefficient matrix $B^L = B^R$ for linear systems for $\boldsymbol{\alpha}^L$ and $\boldsymbol{\alpha}^R$ and the same right-hand sides

$$\boldsymbol{b}^L = \boldsymbol{b}^R = \begin{cases} \dfrac{\partial f}{\partial x}(v_i), & 1 \le i \le 4 \\ \dfrac{\partial^2 f}{\partial x \partial y}(v_{i-4}), & 5 \le i \le 8 \\ \dfrac{\partial^2 f}{\partial x \partial z}(v_{i-8}), & 9 \le i \le 12 \\ \dfrac{\partial^3 f}{\partial x \partial y^2}(v_{i-12}), & 13 \le i \le 16 \\ \dfrac{\partial^3 f}{\partial x \partial y \partial z}(v_{i-16}), & 17 \le i \le 20 \\ \dfrac{\partial^3 f}{\partial x \partial z^2}(v_{i-20}), & 21 \le i \le 24 \\ \dfrac{\partial^4 f}{\partial x \partial y^2 \partial z}(v_{i-24}), & 25 \le i \le 28 \\ \dfrac{\partial^4 f}{\partial x \partial y \partial z^2}(v_{i-28}), & 29 \le i \le 32 \\ \dfrac{\partial^5 f}{\partial x \partial y^2 \partial z^2}(v_{i-32}), & 33 \le i \le 36 \end{cases} \tag{47}$$

Thus, $\boldsymbol{\alpha}^L = \boldsymbol{\alpha}^R$, which implies that $\frac{\partial \mathcal{P}^L}{\partial x}(1,y,z) = \frac{\partial \mathcal{P}^R}{\partial x}(0,y,z)$ and hence $\frac{\partial \mathcal{P}}{\partial x}$ is continuous on the boundary (v_1, v_3, v_4, v_2). □

Corollary 3.2. *The polynomial $\frac{\partial \mathcal{P}}{\partial s}$, $s \in \{x,y,z\}$ is continuous on mesh boundaries perpendicular to the s-axis.*

Proof. From Lemma 3 $\frac{\partial \mathcal{P}}{\partial x}$ is continuous on the boundary (v_1, v_3, v_4, v_2). The boundary is an arbitrary boundary perpendicular to the x-axis, thus $\frac{\partial \mathcal{P}}{\partial x}$ is continuous on any mesh boundary perpendicular to the x-axis. Then, by symmetry and Lemma 3, $\frac{\partial \mathcal{P}}{\partial y}$ and $\frac{\partial \mathcal{P}}{\partial z}$ are continuous on any mesh boundary perpendicular to the y and z-axes respectively. □

Theorem 4 (*Global $\mathcal{C}^1$ Continuity*)**.** *The triquintic interpolant $\mathcal{P}$ is $\mathcal{C}^1$ continuous everywhere.*

Proof. From Corollaries 3.2 and 2.1, the first derivatives of $\mathcal{P}$ are continuous on any mesh boundary perpendicular to the x, y and z axes, thus $\mathcal{P}$ is everywhere $\mathcal{C}^1$ continuous. □

Lemma 5. *The derivatives*

$$\frac{\partial^2 \mathcal{P}}{\partial x \partial y} \text{ and } \frac{\partial^2 \mathcal{P}}{\partial x \partial z}$$

are continuous on mesh boundaries perpendicular to the x-axis.

Proof. From Lemma 3 and Corollary 3.2, $\frac{\partial \mathcal{P}}{\partial x}$ is a polynomial in y and z and continuous on mesh boundaries perpendicular to the x-axis. Thus all derivatives in y and z are also continuous on these boundaries. Specifically, $\frac{\partial^2 \mathcal{P}}{\partial x \partial y}$ and $\frac{\partial^2 \mathcal{P}}{\partial x \partial z}$ are continuous on mesh boundaries perpendicular to the x-axis. □

Corollary 5.1. *The derivatives*

$$\frac{\partial^2 \mathcal{P}}{\partial x \partial y} \text{ and } \frac{\partial^2 \mathcal{P}}{\partial y \partial z}$$

are continuous on mesh boundaries perpendicular to the y-axis and

$$\frac{\partial^2 \mathcal{P}}{\partial x \partial z} \text{ and } \frac{\partial^2 \mathcal{P}}{\partial y \partial z}$$

are continuous on mesh boundaries perpendicular to the z-axis.

Proof. The corollary follows from Lemma 5 and symmetry. □

Lemma 6. *The mixed second derivatives are globally continuous.*

Proof. Lemma 2, Corollary 2.1, Lemma 5 and Corollary 5.1 together prove that the mixed derivatives are continuous on all boundaries and hence are globally continuous. □

Lemma 7. *The polynomial* $\frac{\partial^2 \mathcal{P}}{\partial x^2}$ *is continuous on the boundary* (v_1, v_3, v_4, v_2).

Proof. The proof is similar to that for Lemmas 1 and 3. It is sufficient to show that $\frac{\partial^2 \mathcal{P}^L}{\partial x^2}(1, y, z) = \frac{\partial^2 \mathcal{P}^R}{\partial x^2}(0, y, z)$. Note that

$$\frac{\partial^2 \mathcal{P}}{\partial x^2}(x, y, z) = \sum_{j,k=0}^{5} \sum_{2=1}^{5} i(i-1) a_{ijk} x^{i-2} y^j z^k. \tag{48}$$

On the boundary,

$$\frac{\partial^2 \mathcal{P}^L}{\partial^2 x}(1, y, z) = \sum_{j,k=0}^{5} \left(\sum_{i=2}^{5} i(i-1) a_{ijk} \right) y^j z^k = \left(\boldsymbol{\alpha}^L\right)^T \boldsymbol{\mu}^L, \tag{49}$$

where

$$\alpha^L_{1+j+6k} = \sum_{i=2}^{5} i(i-1) a_{ijk}, \qquad j, k = 0, 1, 2, 3, 4, 5, \tag{50}$$

and

$$\frac{\partial^2 \mathcal{P}^R}{\partial x^2}(0, y, z) = \sum_{j,k=0}^{5} 2a_{2jk}\, y^j z^k = \left(\boldsymbol{\alpha}^R\right)^T \boldsymbol{\mu}^R, \tag{51}$$

with

$$\alpha^R_{1+j+6k} = 2a_{2jk}, \qquad j, k = 0, 1, 2, 3, 4, 5, \tag{52}$$

and

$$\mu^L_{1+j+6k} = \mu^R_{1+j+6k} = y^j z^k, \qquad j, k = 0, 1, 2, 3, 4, 5. \tag{53}$$

Again, we have $\boldsymbol{\mu}^L = \boldsymbol{\mu}^R$, hence we only need to show that $\boldsymbol{\alpha}^L = \boldsymbol{\alpha}^R$. At the four vertices $\{v_1, v_2, v_3, v_4\}$, we enforce the following subset of the original set of constraints

$$\left\{ \frac{\partial^2 \mathcal{P}}{\partial x^2} = \frac{\partial^2 f}{\partial x^2}, \frac{\partial^3 \mathcal{P}}{\partial x^2 \partial y} = \frac{\partial^3 f}{\partial x^2 \partial y}, \frac{\partial^3 \mathcal{P}}{\partial x^2 \partial z} = \frac{\partial^3 f}{\partial x^2 \partial z}, \frac{\partial^4 \mathcal{P}}{\partial x^2 \partial y^2} = \frac{\partial^4 f}{\partial x^2 \partial y^2}, \frac{\partial^4 \mathcal{P}}{\partial x^2 \partial y \partial z} = \frac{\partial^4 f}{\partial x^2 \partial y \partial z}, \right. \\ \left. \frac{\partial^4 \mathcal{P}}{\partial x^2 \partial z^2} = \frac{\partial^4 f}{\partial x^2 \partial z^2}, \frac{\partial^5 \mathcal{P}}{\partial x^2 \partial y^2 \partial z} = \frac{\partial^5 f}{\partial x^2 \partial y^2 \partial z}, \frac{\partial^5 \mathcal{P}}{\partial x^2 \partial y \partial z^2} = \frac{\partial^5 f}{\partial x^2 \partial y \partial z^2}, \frac{\partial^6 \mathcal{P}}{\partial x^2 \partial y^2 \partial z^2} = \frac{\partial^6 f}{\partial x^2 \partial y^2 \partial z^2} \right\}. \tag{54}$$

which involve a double derivative in x. This leads to the same coefficient matrix $B^L = B^R$ for linear systems for $\boldsymbol{\alpha}^L$ and $\boldsymbol{\alpha}^R$ and the same right-hand sides

$$\boldsymbol{b}^L = \boldsymbol{b}^R = \begin{cases} \frac{\partial^2 f}{\partial x^2}(v_i), & 1 \le i \le 4 \\ \frac{\partial^3 f}{\partial x^2 \partial y}(v_{i-4}), & 5 \le i \le 8 \\ \frac{\partial^3 f}{\partial x^2 \partial z}(v_{i-8}), & 9 \le i \le 12 \\ \frac{\partial^4 f}{\partial x^2 \partial y^2}(v_{i-12}), & 13 \le i \le 16 \\ \frac{\partial^4 f}{\partial x^2 \partial y \partial z}(v_{i-16}), & 17 \le i \le 20 \\ \frac{\partial^4 f}{\partial x^2 \partial z^2}(v_{i-20}), & 21 \le i \le 24 \\ \frac{\partial^5 f}{\partial x^2 \partial y^2 \partial z}(v_{i-24}), & 25 \le i \le 28 \\ \frac{\partial^5 f}{\partial x^2 \partial y \partial z^2}(v_{i-28}), & 29 \le i \le 32 \\ \frac{\partial^6 f}{\partial x^2 \partial y^2 \partial z^2}(v_{i-32}), & 33 \le i \le 36 \end{cases} \tag{55}$$

Thus, $\boldsymbol{\alpha}^L = \boldsymbol{\alpha}^R$, which implies that $\frac{\partial^2 \mathcal{P}^L}{\partial x^2}(1, y, z) = \frac{\partial^2 \mathcal{P}^R}{\partial x^2}(0, y, z)$ and hence $\frac{\partial^2 \mathcal{P}}{\partial x^2}$ is continuous on the boundary (v_1, v_3, v_4, v_2). □

Lemma 8. *The polynomial $\frac{\partial^2 \mathcal{P}}{\partial x^2}$ is continuous everywhere.*

Proof. Lemma 7 shows that $\frac{\partial^2 \mathcal{P}}{\partial x^2}$ is continuous on faces perpendicular to the x-axis. Corollary 2.1 shows that $\frac{\partial^2 \mathcal{P}}{\partial x^2}$ is continuous on faces perpendicular to the y and z-axis. Within a mesh element, $\mathcal{P}$ is $\mathcal{C}^\infty$, thus $\frac{\partial^2 \mathcal{P}}{\partial x^2}$ is continuous everywhere. □

Theorem 9 (*Global $\mathcal{C}^2$ Continuity*)**.** *The triquintic interpolant $\mathcal{P}$ is $\mathcal{C}^2$ continuous everywhere.*

Proof. From Lemma 8 and symmetry, $\frac{\partial^2 \mathcal{P}}{\partial x^2}$, $\frac{\partial^2 \mathcal{P}}{\partial y^2}$ and $\frac{\partial^2 \mathcal{P}}{\partial z^2}$ are continuous everywhere. And the mixed second derivatives are continuous everywhere, according to Lemma 6. Thus, $\mathcal{P}$ has global $\mathcal{C}^2$ continuity. □

4.2. Global $\mathcal{C}^3$ continuity does not hold

Theorem 10. *The triquintic interpolant $\mathcal{P}$ is not $\mathcal{C}^3$ continuous everywhere.*

Proof. We prove by contradiction. Consider the interpolant along the x-axis ($y = z = 0$). Without loss of generality, we focus on two adjacent mesh elements on the interval $[0, 2]$ where the left mesh is on $[0, 1]$ and the right mesh is on $[1, 2]$. Define the left interpolant as

$$\mathcal{P}^L(x, 0, 0) = a_{000} + a_{100}x + a_{200}x^2 + a_{300}x^3 + a_{400}x^4 + a_{500}x^5, \tag{56}$$

and the right interpolant as

$$\mathcal{P}^R(x, 0, 0) = b_{000} + b_{100}x + b_{200}x^2 + b_{300}x^3 + b_{400}x^4 + b_{500}x^5. \tag{57}$$

The left and right interpolants are fully determined by the values of the function and its first and second derivatives in x at the endpoints of the intervals $[0, 1]$ and $[1, 2]$ respectively. We find that

$$a_{000} = f(0, 0, 0),\ a_{100} = f_x(0, 0, 0),\ a_{200} = \frac{1}{2} f_{xx}(0, 0, 0), \tag{58}$$

$$\begin{bmatrix} a_{300} \\ a_{400} \\ a_{500} \end{bmatrix} = \begin{bmatrix} 10 & -4 & 1/2 \\ -15 & 7 & -1 \\ 6 & -3 & 1/2 \end{bmatrix} \begin{bmatrix} f(1,0,0) - f(0,0,0) - f_x(0,0,0) - \frac{1}{2}f_{xx}(0,0,0) \\ f_x(1,0,0) - f_x(0,0,0) - f_{xx}(0,0,0) \\ f_{xx}(1,0,0) - f_{xx}(0,0,0) \end{bmatrix}, \tag{59}$$

$$b_{000} = f(1,0,0),\ b_{100} = f_x(1,0,0),\ a_{200} = \frac{1}{2}f_{xx}(1,0,0), \tag{60}$$

$$\begin{bmatrix} b_{300} \\ b_{400} \\ b_{500} \end{bmatrix} = \begin{bmatrix} 10 & -4 & 1/2 \\ -15 & 7 & -1 \\ 6 & -3 & 1/2 \end{bmatrix} \begin{bmatrix} f(2,0,0) - f(1,0,0) - f_x(1,0,0) - \frac{1}{2}f_{xx}(1,0,0) \\ f_x(2,0,0) - f_x(1,0,0) - f_{xx}(1,0,0) \\ f_{xx}(2,0,0) - f_{xx}(1,0,0) \end{bmatrix}. \tag{61}$$

Assume that the interpolant is $\mathcal{C}^3$ continuous everywhere. Then, specifically,

$$\frac{\partial^3 \mathcal{P}^L}{\partial x^3}(1,0,0) = \frac{\partial^3 \mathcal{P}^R}{\partial x^3}(0,0,0), \tag{62}$$

which implies that,

$$a_{300} + 4a_{400} + 5a_{500} = b_{300}. \tag{63}$$

From Eq. (59),

$$\begin{aligned} a_{300} + 4a_{400} + 5a_{500} = 10(f(1,0,0) - f(0,0,0)) \\ -4f_x(0,0,0) - 6f_x(1,0,0) - \frac{1}{2}f_{xx}(0,0,0) + \frac{3}{2}f_{xx}(1,0,0), \end{aligned} \tag{64}$$

and from Eq. (61),

$$b_{300} = 10(f(2,0,0) - f(1,0,0)) - 6f_x(1,0,0) - 4f_x(2,0,0) - \frac{19}{2}f_{xx}(1,0,0) + \frac{1}{2}f_{xx}(2,0,0). \tag{65}$$

Note that because the interpolant is $\mathcal{C}^2$ continuous everywhere,

$$a_{000} = b_{000}, \quad a_{100} = b_{100}, \quad \text{and} \quad a_{200} = b_{200}. \tag{66}$$

Then the consequence of Eqs. (58), (60) and (63) is that, for every interpolated function,

$$4(f_x(2,0,0) - f_x(0,0,0)) - \frac{1}{2}(f_{xx}(2,0,0) - 21f_{xx}(0,0,0)) = 10(f(2,0,0) - f(0,0,0)), \tag{67}$$

which is false. Thus, the triquintic is not globally $\mathcal{C}^3$ continuous. □

5. Error analysis and numerical results

First, we prove that for the tricubic interpolant, the uniform error decays as a quartic and for the triquintic interpolant, the error decays as a sextic. Along the way, we show that the pointwise error decay for the tricubic is quadratic and for the triquintic it is cubic.

5.1. Error analysis

Theorem 11. *For a cubic mesh of length x, the error for the tricubic interpolant decays uniformly as $\mathcal{O}(x^4)$ and the error for the triquintic interpolant decays uniformly as $\mathcal{O}(x^6)$.*

Proof. Let $f(x,y,z) \in \mathcal{C}^\infty$ be the function to be interpolated. Then, the Taylor series for f centered at the origin $\mathbf{0} = (0,0,0)$ is

$$f(x,y,z) = \sum_{i,j,k=0}^{\infty} \frac{1}{i!j!k!} \frac{\partial^{i+j+k} f}{\partial x^i y^j z^k}\Big|_{(0,0,0)} x^i y^j z^k. \tag{68}$$

Define the tricubic interpolant as

$$\mathcal{P}_3(x,y,z) = \sum_{i,j,k=0}^{3} a_{ijk} x^i y^j z^k, \tag{69}$$

and the triquintic interpolant as

$$\mathcal{P}_5(x,y,z) = \sum_{i,j,k=0}^{5} b_{ijk} x^i y^j z^k. \tag{70}$$

Apply the tricubic constraints given in Eq. (4) at $(0,0,0)$ to compute 8 of the coefficients of $\mathcal{P}_3$. Similarly, apply the triquintic contraints in (9), (22), (23), (24) and (25) at $(0,0,0)$ to compute 27 of the coefficients of $\mathcal{P}_5$. We find that

$$a_{ijk} = \frac{\partial^{i+j+k} f}{\partial x^i \partial y^j \partial z^k}\Big|_{(0,0,0)}, \quad i,j,k = 0,1, \tag{71}$$

$$b_{i,j,k} = \frac{1}{i!j!k!}\frac{\partial^{i+j+k} f}{\partial x^i \partial y^j \partial z^k}\Big|_{(0,0,0)}, \quad i,j,k = 0,1,2. \tag{72}$$

Then the residual for the tricubic is given as

$$\begin{aligned} r_3(x,y,z) &= f(x,y,z) - \mathcal{P}_3(x,y,z), \\ &= \frac{1}{2}\left((f_{xx}(\mathbf{0}) - 2a_{200})x^2 + (f_{yy}(\mathbf{0}) - 2a_{020})y^2 + (f_{zz} - 2a_{002})z^2\right) \\ &\quad + \sum_{i+j+k=3}\left(\frac{1}{i!j!k!}\frac{\partial^{i+j+k} f}{\partial x^i y^j z^k}\Big|_{(0,0,0)} - a_{ijk}\right)x^i y^j z^k + \mathcal{O}(x^4), \end{aligned} \tag{73}$$

and the associated uniform error is defined as

$$\max_x |r_3(x,y,z)| = \max_x |f(x,y,z) - \mathcal{P}_3(x,y,z)|. \tag{74}$$

Note that the coefficient

$$a_{200} = 3f(1,0,0) - 3f(0,0,0) - 2f_x(0,0,0) - f_x(1,0,0), \tag{75}$$

which is not necessarily equal to $\frac{1}{2}f_{xx}(\mathbf{0})$. Similarly, a_{020} and a_{002} are not necessarily equal to $\frac{1}{2}f_{yy}(\mathbf{0})$ and $\frac{1}{2}f_{zz}(\mathbf{0})$ respectively. Thus, the pointwise error in a tricubic interpolation given by

$$\begin{aligned} e_3(x,y,z) &= |f(x,y,z) - \mathcal{P}_3(x,y,z)|, \\ &= \left|\frac{1}{2}\left((f_{xx}(\mathbf{0}) - 2a_{200})x^2 + (f_{yy}(\mathbf{0}) - 2a_{020})y^2 + (f_{zz} - 2a_{002})z^2\right) + \cdots\right|, \end{aligned} \tag{76}$$

decays quadratically.

To prove that the uniform error for the tricubic decays as $\mathcal{O}(x^4)$, we need to show that, at a minimum, the coefficients of the quadratic and cubic terms in $r_3(x,y,z)$ behave as $\mathcal{O}(x^2)$ and $\mathcal{O}(x)$ respectively. We do this by expanding the function values such as in Eq. (75) around $(0,0,0)$. In Appendix A, we show that

$$\frac{1}{2!}f_{xx}(\mathbf{0}) - a_{200} = \mathcal{O}(x^3), \quad \frac{1}{2!}f_{xxy}(\mathbf{0}) - a_{210} = \mathcal{O}(x^2), \quad \frac{1}{3!}f_{xxx}(\mathbf{0}) - a_{300} = \mathcal{O}(x^3).$$

By symmetry, similar relationships hold for the other coefficients of the quadratic and cubic terms. Thus,

$$\max_x |f(x,y,z) - \mathcal{P}_3(x,y,z)| = \mathcal{O}(x^4), \tag{77}$$

where we have also used $a_{111} = f_{xyz}(\mathbf{0})$ given by Eq. (71).

We follow similar arguments for the triquintic interpolant with the residual given as

$$\begin{aligned} r_5(x,y,z) &= f(x,y,z) - \mathcal{P}_5(x,y,z), \\ &= \frac{1}{6}\left((f_{xxx}(\mathbf{0}) - 6b_{300})x^3 + (f_{yyy}(\mathbf{0}) - 6b_{030})y^3 + (f_{zzz} - 2b_{003})z^3\right) \\ &\quad + \sum_{4\le i+j+k\le 5}\left(\frac{1}{i!j!k!}\frac{\partial^{i+j+k} f}{\partial x^i y^j z^k}\Big|_{(0,0,0)} - a_{ijk}\right)x^i y^j z^k + \mathcal{O}(x^6), \end{aligned} \tag{78}$$

and

$$\max_x |r_5(x,y,z)| = \max_x |f(x,y,z) - \mathcal{P}_5(x,y,z)|, \tag{79}$$

defines the triquintic uniform error. Note that, Eq. (15) and Eq. (20), imply

$$b_{300} = 10(f(1,0,0) - f(0,0,0)) - 6f_x(0,0,0) - 4f_x(1,0,0) - \frac{3}{2}f_{xx}(0,0,0) + \frac{1}{2}f_{xx}(1,0,0), \tag{80}$$

which is not necessarily equal to $\frac{1}{6}f_{xxx}(\mathbf{0})$. Similarly, b_{030} and b_{003} are not necessarily equal to $\frac{1}{6}f_{yyy}(\mathbf{0})$ and $\frac{1}{6}f_{zzz}(\mathbf{0})$ respectively. Thus, the pointwise error in the triquintic interpolation given by

$$\begin{aligned} e_5(x,y,z) &= |f(x,y,z) - \mathcal{P}_5(x,y,z)|, \\ &= \left|\frac{1}{6}\left((f_{xxx}(\mathbf{0}) - 6b_{300})x^3 + (f_{yy}(\mathbf{0}) - 6b_{030})y^3 + (f_{zz} - 6b_{003})z^3\right) + \cdots\right|, \end{aligned} \tag{81}$$

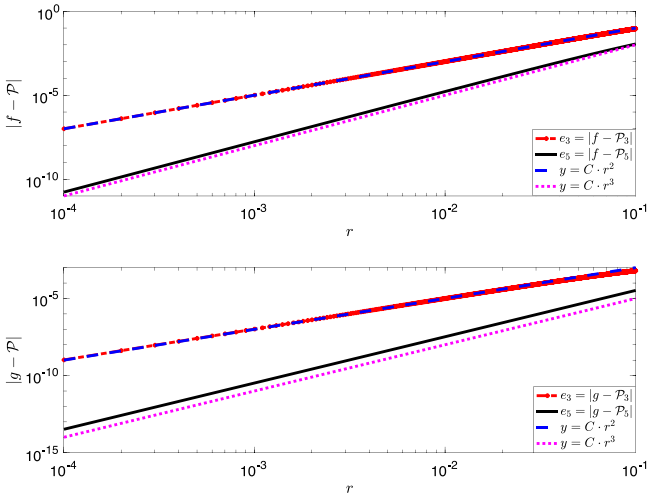

Fig. 3. Numerical evidence for decay rate of the pointwise errors for the tricubic and triquintic interpolants. The top plot is for $f(x, y, z)$ and the bottom plot is for $g(x, y, z)$.

decays as a cubic.

We need to show that the coefficients of the cubic, quartic and quintic terms in $r_5(x, y, z)$ behave as $\mathcal{O}(x^3)$, $\mathcal{O}(x^2)$ and $\mathcal{O}(x)$ respectively in order to prove that the error for the triquintic decays uniformly as $\mathcal{O}(x^6)$. We do this by expanding the function values, such as in Eq. (80) around (0, 0, 0). In Appendix B, we show that

$$\frac{1}{3!}f_{xxx}(\mathbf{0}) - b_{300} = \mathcal{O}(x^4),$$

$$\frac{1}{4!}f_{xxxx}(\mathbf{0}) - b_{400} = \mathcal{O}(x^4), \quad \frac{1}{3!}f_{xxxy} - b_{310} = \mathcal{O}(x^3),$$

$$\frac{1}{5!}f_{xxxxx}(\mathbf{0}) - b_{500} = O(x^4), \quad \frac{1}{4!}f_{xxxxy}(\mathbf{0}) - b_{410} = O(x^3), \quad \frac{1}{3!}f_{xxxyy}(\mathbf{0}) - b_{320} = O(x^2),$$

$$\frac{1}{3!}f_{xxxyz}(\mathbf{0}) - b_{311} = O(x^2).$$

Again, by symmetry, similar relationships hold for the other coefficients of the quadratic, cubic and quartic terms of the residual. Thus,

$$\max_x |f(x, y, z) - \mathcal{P}_5(x, y, z)| = \mathcal{O}(x^6), \tag{82}$$

where we have also used the values for b_{ijk} given by Eq. (72). □

5.2. Numerical results

Fig. 3 provides numerical evidence for pointwise errors given in Eqs. (76) and (81) for $f(x, y, z) = \frac{1}{\sqrt{x^2+y^2+z^2+0.1}}$ (top plot) and $g(x, y, z) = (x^2 + y^2 + z^2) \cdot \mathrm{e}^{-(x^2+y^2+z^2)}$ (bottom plot). The absolute errors are computed along the vector $\mathbf{r} = \gamma\left(\frac{1}{3}, \frac{1}{3}, \frac{1}{3}\right)$, where $\gamma = 0 : 0.001 : 0.1$. Fig. 3 is a log–log plot of the errors vs $r = |\mathbf{r}|$. We see that the absolute error for the tricubic, $e_3(x, y, z)$, matches $y = C \cdot r^2$ to support the conclusion in Eq. (76). Similarly, the triquintic absolute error, $e_5(x, y, z)$, matches $y = C \cdot r^3$, as predicted by Eq. (81).

Fig. 3 also shows that as expected, the triquintic interpolant is more accurate than the tricubic interpolant. Fig. 4 provides further study of the comparative accuracy of the two interpolants. We plot the error for the interpolation of a function and its derivatives $\{\partial_x, \partial_{xy}, \partial_{xyz}\}$ at 50 randomly generated points in the unit cube. Results are provided for the same two functions, $f(x, y, z)$ (left column) and $g(x, y, z)$ (right column). As expected, triquintic interpolation provides higher accuracy for a function and its derivatives.

Table 1, compares the accuracy of the integrals of the interpolants for $f(x, y, z)$ and $g(x, y, z)$. We use MATLAB's in-built numerical quadrature function to compute $\int_{[0,1]^3} f \, d\mathbf{x}$ and $\int_{[0,1]^3} g \, d\mathbf{x}$. The integral for the interpolants are computed as

$$\int_{[0,1]^3} \mathcal{P} \, d\mathbf{x} = \sum_{i,j,k=0}^{n} \int_{[0,1]^3} a_{ijk} x^i y^j z^k \, \mathbf{dx} = \sum_{i,j,k=0}^{n} \frac{a_{ijk}}{(i+1)(j+1)(k+1)}, \tag{83}$$

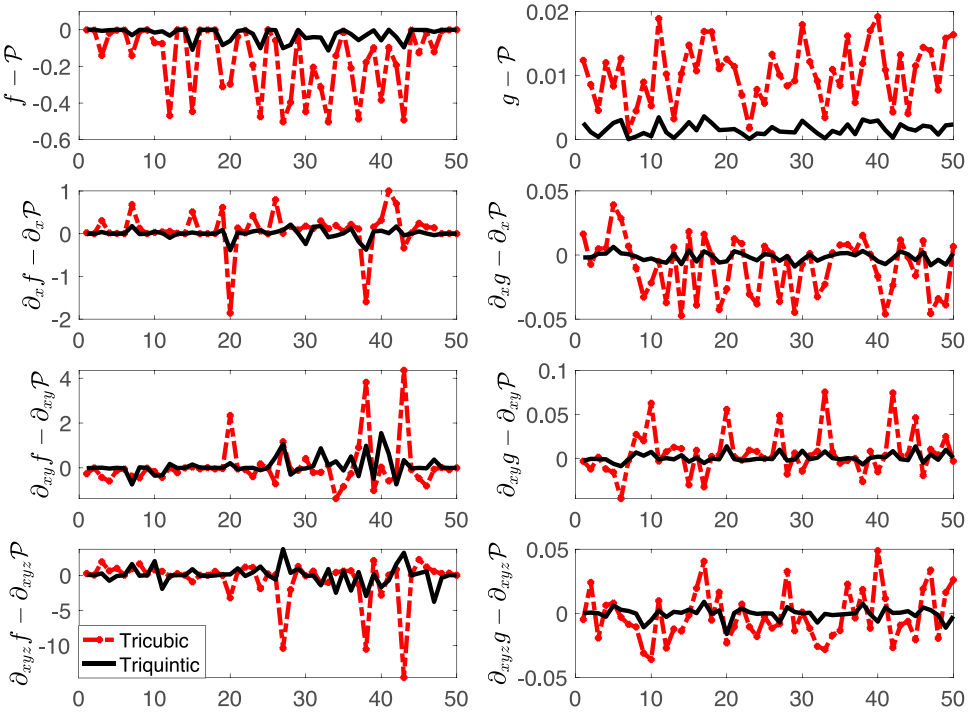

Fig. 4. Comparison of the error in the tricubic and triquintic interpolants for 2 functions and their derivatives. The left column is for $f(x, y, z)$ and the right column is for $g(x, y, z)$.

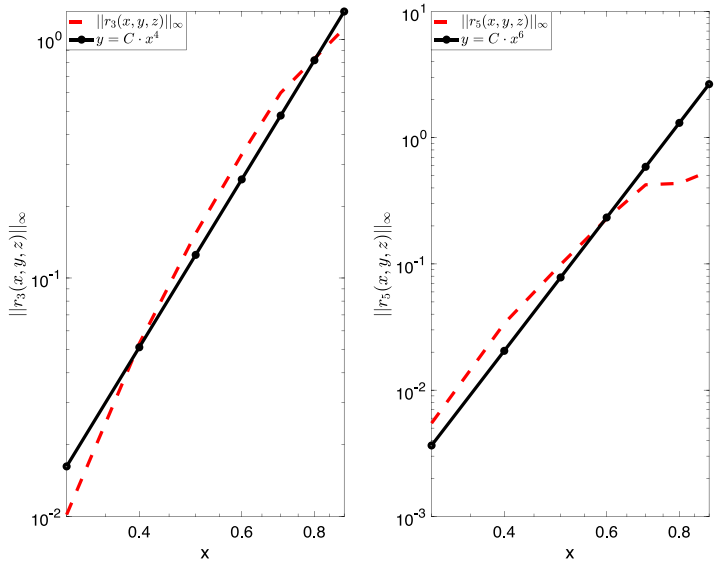

Fig. 5. Numerical evidence for the decay rate of the uniform norm of the errors for the tricubic and triquintic interpolants for $u(x, y, z) = (x^2+y^2+z^2)^3$. The left column is uniform error for the tricubic and the right is the uniform error for the triquintic.

where $n = 3$ for the tricubic and $n = 5$ for the triquintic. Table 1 shows that the triquintic approximation of the integrals is more accurate than the tricubic approximation.

Figs. 5 and 6 provide evidence for the uniform errors given in Eqs. (77) and (82) for the functions $u(x, y, z) = \left(x^2 + y^2 + z^2\right)^3$ and $v(x, y, z) = \left(x^2 + y^2 + z^2\right)^4$. The length of the cube $x = 0.3 : 0.05 : 0.9$. For each length of the cube, the maximum norm of the residual is computed over 100 randomly generated points in the cube. In both Figs. 5 and 6, we see good agreement with the decay rates given in Theorem 11.

Table 1
Accuracy of integrals of the interpolants.

Interpolant	$\int_{[0,1]^3} f(x) - \mathcal{P}(x)\ dx$	$\int_{[0,1]^3} g(x) - \mathcal{P}(x)\ dx$
$\mathcal{P}_3$	0.128868208976672	0.010551038583430
$\mathcal{P}_5$	0.018646565877596	0.001756644668320

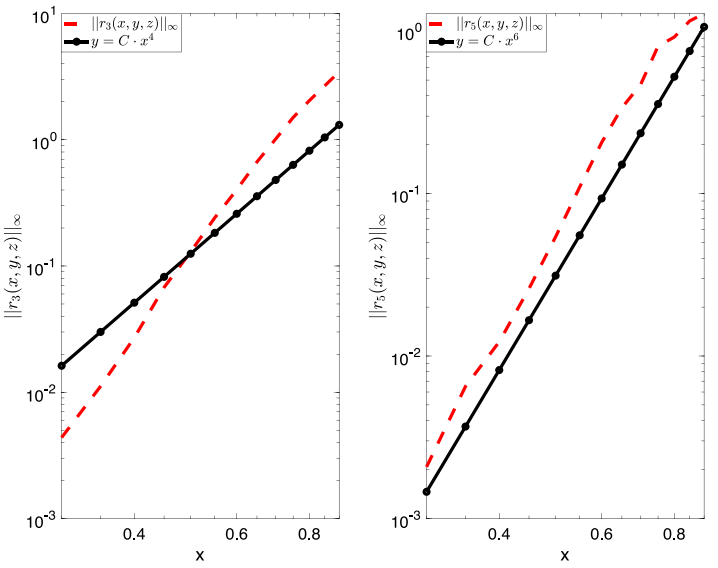

Fig. 6. Numerical evidence for the decay rate of the uniform norm of the errors for the tricubic and triquintic interpolants for $v(x, y, z) = (x^2+y^2+z^2)^4$. The left column is uniform error for the tricubic and the right is the uniform error for the triquintic.

Before we conclude, we note that as explained by Lekien and Marsden, even though the presentation has been focused on Cartesian grids, the development extends to rectilinear grids as well. For a rectilinear mesh unit $[x_{\min}, x_{\max}] \times [y_{\min}, y_{\max}] \times [z_{\min}, z_{\max}]$, the mesh unit is mapped to the unit cube via the transformation

$$T(x, y, z) = \left(\frac{x - x_{\min}}{\Delta x}, \frac{y - y_{\min}}{\Delta y}, \frac{z - z_{\min}}{\Delta z} \right) = (\bar{x}, \bar{y}, \bar{z}), \tag{84}$$

where $\Delta x = x_{\max} - x_{\min}$, $\Delta y = y_{\max} - y_{\min}$ and $\Delta z = z_{\max} - z_{\min}$. Then, the triquintic interpolant is defined as

$$\mathcal{P}(x, y, z) = \sum_{i,j,k=0}^{5} a_{ijk} \bar{x}^i \bar{y}^j \bar{z}^k. \tag{85}$$

The elements of the right-hand side vector $\boldsymbol{b}$ defined in Eq. (26) are scaled accordingly as

$$\Delta x^\beta \Delta y^\gamma \Delta z^\nu \frac{\partial^{\beta+\gamma+\nu} f}{\partial x^\beta \partial y^\gamma \partial z^\nu}, \qquad \beta, \gamma, \nu \in \{0, 1, 2\}. \tag{86}$$

6. Conclusions

This paper developed an isotropic triquintic interpolant and proved that the interpolant is $\mathcal{C}^2$ continuous everywhere. The driver of the interpolation method is a 216 × 216 invertible matrix that relates the coefficients of the interpolant to the function and its derivatives at the eight corners of a unit cube mesh element. We proved that the method is not $\mathcal{C}^3$ continuous globally and that the error decays as a cubic. Numerical tests were provided to support the analysis of the convergence of the method. The advantages of the triquintic interpolant developed in this paper over the tricubic interpolant of Lekien and Marsden [9] are:

(1) The triquintic is $\mathcal{C}^2$ everywhere and thus has higher smoothness while the tricubic is globally $\mathcal{C}^1$.
(2) The triquintic is more accurate than the tricubic for approximating function values.
(3) The triquintic produces more accurate interpolation of higher order derivatives.

The disadvantage of the triquintic is that it requires up to 6th order derivatives of the interpolated function while the tricubic requires only up to 3rd order derivatives. Additionally, the tricubic matrix is 64 × 64 while the triquintic matrix

is 216 × 216. This disparity in matrix sizes will perhaps be an issue if the matrix–vector multiplication has to be done many times. However, the best use case for both interpolants is when several values inside the unit cube need to be interpolated. Then the coefficients of the interpolant are computed once by Eq. (5) and used repeatedly to interpolate all the needed values. In this case, the difference in computational cost between the tricubic and triquintic interpolants are negligible.

Data availability

The data for this work is publicly available on GitHub and the link is provided as reference 12 in the paper.

Acknowledgments

This work was partially supported by National Science Foundation, United States grant CHE-2016048 and start-up funds from San Francisco State University, United States.

Appendix A. Asymptotic behavior of coefficients of the tricubic interpolant residual

A.1. Behavior of $\left(\frac{1}{2!}f_{xx}(\mathbf{0}) - a_{200}\right)$

Eq. (75) defines

$$a_{200} = 3f(1,0,0) - 3f(\mathbf{0}) - 2f_x(\mathbf{0}) - f_x(1,0,0). \tag{A.1}$$

Expand both $f(1,0,0)$ and $f_x(1,0,0)$ as a Taylor series around $\mathbf{0}$ to get

$$f(1,0,0) = f(\mathbf{0}) + f_x(\mathbf{0}) + \frac{1}{2}f_{xx}(\mathbf{0}) + \frac{1}{6}f_{xxx}(\mathbf{0}) + \mathcal{O}(x^4), \tag{A.2}$$

$$f_x(1,0,0) = f_x(\mathbf{0}) + f_{xx}(\mathbf{0}) + \frac{1}{2}f_{xxx}(\mathbf{0}) + \mathcal{O}(x^3). \tag{A.3}$$

Then, put Eqs. (A.2) and (A.3) into Eq. (A.1), to get

$$a_{200} = \frac{1}{2!}f_{xx}(\mathbf{0}) + \mathcal{O}(x^3). \tag{A.4}$$

Then we get,

$$\frac{1}{2!}f_{xx}(\mathbf{0}) - a_{200} = \mathcal{O}(x^3).$$

A.2. Behavior of $\left(\frac{1}{2!}f_{xxy}(\mathbf{0}) - a_{210}\right)$

We apply one of the tricubic constraints from Eq. (4) to first evaluate

$$\left.\frac{\partial^2 \mathcal{P}_3}{\partial x \partial y}\right|_{(1,0,0)} = a_{110} + 2a_{210} = f_{xy}(1,0,0). \tag{A.5}$$

Recall, from Eq. (71), that $a_{110} = f_{xy}(\mathbf{0})$. Then,

$$a_{210} = \frac{1}{2}\left(f_{xy}(1,0,0) - f_{xy}(\mathbf{0})\right). \tag{A.6}$$

Expand $f_{xy}(1,0,0)$ about the origin to get

$$f_{xy}(1,0,0) = f_{xy}(\mathbf{0}) + f_{xxy}(\mathbf{0}) + \mathcal{O}(x^2). \tag{A.7}$$

Then from Eqs. (A.6) and (A.7),

$$a_{210} = \frac{1}{2!}f_{xxy}(\mathbf{0}) + \mathcal{O}(x^2), \tag{A.8}$$

thus,

$$\frac{1}{2!}f_{xxy}(\mathbf{0}) - a_{210} = \mathcal{O}(x^2).$$

A.3. Behavior of $\left(\frac{1}{3!}f_{xxx}(\mathbf{0}) - a_{300}\right)$

First note that

$$f(1,0,0) = f(\mathbf{0}) + f_x(\mathbf{0}) + a_{200} + a_{300}, \tag{A.9}$$

and

$$\left.\frac{\partial f}{\partial x}\right|_{(1,0,0)} = f_x(\mathbf{0}) + 2a_{200} + 3a_{300} = f_x(1,0,0). \tag{A.10}$$

This implies that

$$a_{300} = f_x(1,0,0) - 2f(1,0,0) + f_x(\mathbf{0}) + 2f(\mathbf{0}). \tag{A.11}$$

Using the expansions for $f(1,0,0)$ and $f_x(1,0,0)$ in Eqs. (A.2) and (A.3) we see that

$$a_{300} = \frac{1}{3!}f_{xxx}(\mathbf{0}) + \mathcal{O}(x^3). \tag{A.12}$$

Thus,

$$\frac{1}{3!}f_{xxx}(\mathbf{0}) - a_{300} = \mathcal{O}(x^3).$$

Appendix B. Asymptotic behavior of coefficients of the triquintic interpolant

B.1. Behavior of $\left(\frac{1}{3!}f_{xxx}(\mathbf{0}) - b_{300}\right)$

From the constraints for the triquintic interpolant, we find that

$$b_{300} = 10(f(1,0,0) - f(0,0,0)) - 6f_x(0,0,0) - 4f_x(1,0,0) - \frac{3}{2}f_{xx}(0,0,0) + \frac{1}{2}f_{xx}(1,0,0). \tag{B.1}$$

Now, expand $f(1,0,0)$, $f_x(1,0,0)$ and $f_{xx}(1,0,0)$ around $(0,0,0)$ to get

$$f(1,0,0) = f(\mathbf{0}) + f_x(\mathbf{0}) + \frac{1}{2}f_{xx}(\mathbf{0}) + \frac{1}{6}f_{xxx}(\mathbf{0}) + \frac{1}{24}f_{xxxx}(\mathbf{0}) + \frac{1}{120}f_{xxxxx}(\mathbf{0}) + \mathcal{O}(x^6), \tag{B.2}$$

$$f_x(1,0,0) = f_x(\mathbf{0}) + f_{xx}(\mathbf{0}) + \frac{1}{2}f_{xxx}(\mathbf{0}) + \frac{1}{6}f_{xxxx}(\mathbf{0}) + \frac{1}{24}f_{xxxxx}(\mathbf{0}) + \mathcal{O}(x^5), \tag{B.3}$$

$$f_{xx}(1,0,0) = f_{xx}(\mathbf{0}) + f_{xxx}(\mathbf{0}) + \frac{1}{2}f_{xxxx}(\mathbf{0}) + \frac{1}{6}f_{xxxxx}(\mathbf{0}) + \mathcal{O}(x^4). \tag{B.4}$$

Put Eqs. (B.2), (B.3) and (B.4) into Eq. (B.1) to get

$$b_{300} = \frac{1}{3!}f_{xxx}(\mathbf{0}) + \mathcal{O}(x^4), \tag{B.5}$$

which shows that

$$\frac{1}{3!}f_{xxx}(\mathbf{0}) - b_{300} = \mathcal{O}(x^4).$$

B.2. Formulas for the b_{400} and b_{500} terms

We apply two of the triquintic constraints at $(1,0,0)$ to generate the equations

$$\left.\frac{\partial \mathcal{P}_5}{\partial x}\right|_{(1,0,0)} = b_{100} + 2b_{200} + 3b_{300} + 4b_{400} + 5b_{500} = f_x(1,0,0), \tag{B.6}$$

$$\left.\frac{\partial^2 \mathcal{P}_5}{\partial x^2}\right|_{(1,0,0)} = 2b_{200} + 6b_{300} + 12b_{400} + 20b_{500} = f_{xx}(1,0,0). \tag{B.7}$$

We know from Eq. (72) that $b_{100} = f_x(\mathbf{0})$, $2b_{200} = f_{xx}(\mathbf{0})$, thus Eqs. (B.6) and (B.7) imply that

$$b_{400} = f_x(1,0,0) - f_x(\mathbf{0}) - \frac{3}{4}f_{xx}(\mathbf{0}) - \frac{1}{4}f_{xx}(1,0,0) - \frac{3}{2}b_{300}, \tag{B.8}$$

and

$$b_{500} = \frac{1}{5}\left(f_{xx}(1,0,0) + 2f_{xx}(\mathbf{0}) - 3f_x(1,0,0) + 3f_x(\mathbf{0}) + 3b_{300}\right). \tag{B.9}$$

B.3. Behavior of $\left(\frac{1}{4!}f_{xxxx}(\mathbf{0}) - b_{400}\right)$

We insert Eqs. (B.3), (B.4) and (B.5) in Eq. (B.8) to get

$$b_{400} = \frac{1}{4!}f_{xxxx}(\mathbf{0}) + \mathcal{O}(x^4). \tag{B.10}$$

Thus,

$$\frac{1}{4!}f_{xxxx}(\mathbf{0}) - b_{400} = \mathcal{O}(x^4).$$

B.4. Behavior of $\left(\frac{1}{5!}f_{xxxx}(\mathbf{0}) - b_{400}\right)$

We insert Eqs. (B.3), (B.4) and (B.5) in Eq. (B.9) to get

$$b_{500} = \frac{1}{5!}f_{xxxx}(\mathbf{0}) + \mathcal{O}(x^4). \tag{B.11}$$

Thus,

$$\frac{1}{5!}f_{xxxx}(\mathbf{0}) - b_{500} = \mathcal{O}(x^4).$$

B.5. Formulas for the b_{310} *and* b_{410} *terms*

We apply two of the triquintic constraints at $(1, 0, 0)$ to generate the two equations

$$\left.\frac{\partial^2 \mathcal{P}_5}{\partial x \partial y}\right|_{(1,0,0)} = f_{xy}(\mathbf{0}) + 2b_{210} + 3b_{310} + 4b_{410} = f_{xy}(1, 0, 0), \tag{B.12}$$

$$\left.\frac{\partial^3 \mathcal{P}_5}{\partial x^2 \partial y}\right|_{(1,0,0)} = 2b_{210} + 6b_{310} + 12b_{410} = f_{xxy}(1, 0, 0). \tag{B.13}$$

Then using the fact that $2b_{210} = f_{xxy}(\mathbf{0})$, we find that

$$b_{310} = \frac{1}{3}\left(3f_{xy}(1, 0, 0) - 3f_{xy}(\mathbf{0}) - f_{xxy}(1, 0, 0) - 2f_{xxy}(\mathbf{0})\right), \tag{B.14}$$

and

$$b_{410} = \frac{1}{4}\left(f_{xxy}(1, 0, 0) - 2f_{xy}(1, 0, 0) + 2f_{xy}(\mathbf{0}) + f_{xxy}(\mathbf{0})\right). \tag{B.15}$$

B.6. Behavior of $\left(\frac{1}{3!}f_{xxxy}(\mathbf{0}) - b_{310}\right)$

Now expand $f_{xy}(1, 0, 0)$ and $f_{xxy}(1, 0, 0)$ about the origin to get

$$f_{xy}(1, 0, 0) = f_{xy}(\mathbf{0}) + f_{xxy}(\mathbf{0}) + \frac{1}{2}f_{xxxy}(\mathbf{0}) + \frac{1}{6}f_{xxxxy} + \mathcal{O}(x^4), \tag{B.16}$$

$$f_{xxy}(1, 0, 0) = f_{xxy}(\mathbf{0}) + f_{xxxy}(\mathbf{0}) + \frac{1}{2}f_{xxxxy}(\mathbf{0}) + \mathcal{O}(x^3). \tag{B.17}$$

Insert Eqs. (B.16) and (B.17) into (B.14) to get

$$b_{310} = \frac{1}{3!}f_{xxxy} + \mathcal{O}(x^3). \tag{B.18}$$

Thus,

$$\frac{1}{3!}f_{xxxy}(\mathbf{0}) - b_{310} = \mathcal{O}(x^3).$$

B.7. Behavior of $\left(\frac{1}{4!}f_{xxxxy}(\mathbf{0}) - b_{410}\right)$

Insert Eqs. (B.16) and (B.17) into (B.15) to get

$$b_{410} = \frac{1}{4!}f_{xxxxy} + \mathcal{O}(x^3). \tag{B.19}$$

Thus,

$$\frac{1}{4!}f_{xxxxy}(\mathbf{0}) - b_{410} = \mathcal{O}(x^3).$$

B.8. Behavior of $\left(\frac{1}{3!2!}f_{xxxyy}(\mathbf{0}) - b_{320}\right)$

Apply one of the triquintic constraints at $(1, 0, 0)$ to get

$$\left.\frac{\partial^4 \mathcal{P}_5}{\partial x^2 \partial y^2}\right|_{(1,0,0)} = 4b_{220} + 12b_{320} = f_{xxyy}(1, 0, 0). \tag{B.20}$$

Expand $f_{xxyy}(1, 0, 0)$ about the origin as

$$f_{xxyy}(1, 0, 0) = f_{xxyy}(\mathbf{0}) + f_{xxxyy}(\mathbf{0}) + \mathcal{O}(x^2), \tag{B.21}$$

and use the fact that $4b_{220} = f_{xxyy}(\mathbf{0})$ to get

$$b_{320} = \frac{1}{3!2!}f_{xxxyy}(\mathbf{0}) + \mathcal{O}(x^2). \tag{B.22}$$

Thus,

$$\frac{1}{3!2!}f_{xxxyy}(\mathbf{0}) - b_{320} = \mathcal{O}(x^2).$$

B.9. Behavior of $\left(\frac{1}{3!}f_{xxxyz}(\mathbf{0}) - b_{311}\right)$

Apply one of the triquintic constraints at $(1, 0, 0)$ to get

$$\left.\frac{\partial^4 \mathcal{P}_5}{\partial x^2 \partial y \partial z}\right|_{(1,0,0)} = 2b_{211} + 6b_{311} = f_{xxyz}(1, 0, 0). \tag{B.23}$$

Expand $f_{xxyz}(1, 0, 0)$ about the origin as

$$f_{xxyz}(1, 0, 0) = f_{xxyz}(\mathbf{0}) + f_{xxxyz}(\mathbf{0}) + \mathcal{O}(x^2), \tag{B.24}$$

and use the fact that $2b_{211} = f_{xxyz}(\mathbf{0})$ to get

$$b_{311} = \frac{1}{3!}f_{xxxyz}(\mathbf{0}) + \mathcal{O}(x^2). \tag{B.25}$$

Thus,

$$\frac{1}{3!}f_{xxxyz}(\mathbf{0}) - b_{311} = \mathcal{O}(x^2).$$

References

[1] F. Lekien, C. Coulliette, J. Marsden, Lagrangian structures in very high-frequency radar data and optimal pollution timing, in: American Institute of Physics Conference Proceedings, Vol. 676, 2003, pp. 162–168.
[2] Q.R. Marksteiner, The use of tricubic interpolation with spectral derivatives to integrate particle trajectories in complicated electromagnetic fields, J. Comput. Phys. 229 (2010) 6688–6695.
[3] A. Kadosh, D. Cohen-Or, R. Yagel, Tricubic interpolation of discrete surfaces for binary volumes, IEEE Trans. Vis. Comput. Graph. 9 (4) (2003) 580–586.
[4] J.C. Bernauer, J. Diefenbach, G. Elbakian, G. Gavrilov, N. Goerrissen, D.K. Hasell, B.S. Henderson, Y. Holler, G. Karyan, J. Ludwig, H. Marukyan, Y. Naryshkin, C. O'Connor, R.L. Russell, A. Schmidt, U. Schneekloth, K. Suvorov, D. Veretennikov, Measurement and tricubic interpolation of the magnetic field for the OLYMPUS experiment, Nucl. Instrum. Methods Phys. Res. A 823 (2016) 9–14.
[5] C. Katan, R. Rabiller, C. Lecomte, M. Guezo, V. Oison, M. Souhassou, Numerical computation of critical properties and atomic basins from three-dimensional grid electron densities, J. Appl. Crystallogr. 36 (2003) 65–73.
[6] D. Dubbeldam, S. Calero, D.E. Ellis, R.Q. Snurr, RASPA: molecular simulation software for adsorption and diffusion in flexible nanoporous materials, Mol. Simul. 42 (2) (2016) 81–101.
[7] H.A. Boateng, S. Tlupova, The effect of global smoothness on the accuracy of treecodes, Comm. Comp. Phys. (2023) (in print).
[8] P.V. Afonine, B.K. Poon, R.J. Read, O.V. Sobolev, T.C. Terwilliger, A. Urzhumtsev, P.D. Adams, Real-space refinement in PHENIX for cryo-EM and crystallography, Acta Cryst. D74 (2018) 531–544.
[9] F. Lekien, J. Marsden, Tricubic interpolation in three dimensions, Internat. J. Numer. Methods Engrg. 63 (2005) 455–471.
[10] D.K. Ramanah, G. Lavaux, J. Jasche, B.D. Wandelt, Cosmological inference from Bayesian forward modelling of deep galaxy redshift surveys, Astron. Astrophys. 621 (A69) (2019) 1–18.
[11] J. Shi, D. Chopp, J. Lua, N. Sukumar, T. Belytschko, Abaqus implementation of extended finite element method using a level set representation for three-dimensional fatigue crack growth and life predictions, Eng. Fract. Mech. 77 (14) (2010) 2840–2863.
[12] H. Boateng, K. Bradach, Inverse matrix for isotropic triquintic scaled by a factor of 8, 2022, URL https://github.com/krbradach/triquintic/blob/main/scaled_by8_inverse_matrix.csv.
[13] S. Axler, Linear Algebra Done Right, Vol. 3, Springer, 2015.
[14] K. Bradach, A Triquintic Interpolation Method with Global C^2 Continuity, Masters thesis. San Francisco State University, 1600 Holloway Ave, San Francisco CA 94132, 2022.